Vernalization Attenuates Age-Dependent Decline of Glucosinolates in Cabbage (Brassica oleracea ssp. capitata) through Coordinated Transcriptomic and Metabolomic Reprogramming

Heewon Moon
Chung-Ang University
Minkyu Park
EuchroGene LLC
Eojin Cho
Chung-Ang University
Dong-Hwan Kim
dhkim92@cau.ac.kr

Chung-Ang University

Research Article

Keywords: Vernalization, RNA-seq, Cabbage, Brassica oleracea L., Glucosinolates

Posted Date: December 17th, 2025

DOI: https://doi.org/10.21203/rs.3.rs-8223426/v1

Additional Declarations: No competing interests reported.

Version of Record: A version of this preprint was published at BMC Plant Biology on February 9th, 2026. See the published version at https://doi.org/10.1186/s12870-026-08267-6.

Abstract

Vernalization, a prolonged exposure to low temperature occurs in many winter-annual, biennial, and perennial plants and is accompanied by extensive developmental and metabolic reprogramming. Glucosinolates (GSLs) are sulfur- and nitrogen-containing secondary metabolites predominantly found in the Brassicaceae family, where they play crucial roles in defense against abiotic and biotic stresses, while also conferring health benefits to humans due to their anti-carcinogenic and anti-inflammatory properties. To elucidate the impact of vernalization on GSL biosynthesis in cabbage (Brassica oleracea ssp. capitata), we performed integrated transcriptomic and metabolomic analyses in response to vernalization treatment. Metabolite profiling by HPLC revealed that total GSL content decreased progressively with plant age. However, long-term cold exposure during vernalization exerted a positive effect on total GSL accumulation, maintaining higher GSL levels compared to non-vernalized controls. RNA-seq analysis across the vernalization time course showed that more than half of the 78 identified GSL biosynthetic genes exhibited altered expression in response to vernalization. Interestingly, clustering of differentially expressed genes revealed two contrasting groups: (1) Vernalization-Repressed GSL genes (VRGs), corresponding to reduced GSL accumulation, and (2) Vernalization-Induced GSL genes (VIGs), associated with the selective induction of specific GSL compounds. Correlation analyses integrating transcriptomic and metabolite data identified key GSL pathway genes whose expression patterns were significantly correlated with profiles of aliphatic and indolic GSLs throughout vernalization. Collectively, these findings demonstrate that vernalization positively influences GSL accumulation in cabbage, with VRGs and VIGs jointly contributing to the modulation of aliphatic and indolic GSL biosynthesis under prolonged cold conditions.

INTRODUCTION

Cabbage (*Brassica oleracea*) is a leafy vegetable that belongs to the Brassicaceae family, also known as the mustard or cruciferous family. It is one of the most widely cultivated and consumed vegetables around the world. Cabbage grows best in cool weather, making it a popular crop in temperate regions. It is usually grown as an annual vegetable, though it is a biennial plant, meaning it completes its life cycle in two years if allowed to flower and set seeds. Cabbage requires a process known as *vernalization* to acquire the competence to flower(Amasino, 2004). Vernalization, exposure to a prolonged cold period enables cabbage to undergo physiological changes that allow it to acquire the competence to flower.

Cabbage, like other members of the Brassicaceae family, is rich in these sulfur-containing compounds, which contribute to its characteristic flavor and its ability to deter pests. Glucosinolates (GSLs) are key secondary metabolites found in the Brassicaceae family plants, which play a crucial role in both plant defense and human health (Grubb and Abel, 2006; Clay et al., 2009; Mi ekus et al., 2020). GSLs serve as a chemical defense system. When cabbage is damaged, such as during herbivore attack or mechanical injury, an enzyme called myrosinase is activated. This enzyme breaks down GSLs into another bioactive compounds, primarily isothiocyanates, which are toxic or deterrent to pests and pathogens (Bell et al., 2018). The production and variety of GSLs in cabbage can vary depending on endogenous factors (i.e.

developmental stage) and environmental conditions (i.e. nutrient availability, temperature, and stress) (Grubb and Abel, 2006; Yan and Chen, 2007; Hopkins et al., 2009). This variability helps cabbage adapt to its surroundings, optimizing its defense mechanisms. GSLs in cabbage are more than just defense chemicals; they offer significant potential for human health, especially in terms of cancer prevention and general wellness (Verhoeven et al., 1996; Keck and Finley, 2004).

Based on the amino acid precursors, GSLs can be grouped into three categories: aliphatic, indolic, and aromatic GSLs (Fahey et al., 2001; Grubb and Abel, 2006; Halkier and Gershenzon, 2006; Petersen et al., 2018). Aliphatic GSLs are derived from alanine, leucine, isoleucine, valine, or methionine, whereas indolic and aromatic GSLs are derived from tryptophan and phenylalanine or tyrosine, respectively (Fig. 1). Studies using Arabidopsis model plant have identified transcription factors and metabolic enzyme genes involved in the GSLs biosynthesis (Sønderby et al., 2010a). For example, a couple of of MYB transcription factors such as MYB28, MYB29, and MYB76 positively control aliphatic GSLs biosynthesis (Hirai et al., 2007; Sønderby et al., 2007; Gigolashvili et al., 2008). Meanwhile, other MYB factors like MYB34, MYB51, and MYB122 are responsible for the regualtion of indolic GSLs biosynthesis (Celenza et al., 2005; Gigolashvili et al., 2007; Malitsky et al., 2008). These MYB TFs seems to regulate downstream biosynthetic genes involved in the GSLs biosynthesis. Aliphatic GSLs biosynthesis are mainly made up of three stages like ‘chain elongation’ stage, ‘core structure formation’ stage, ‘secondary modification’ stage(Sønderby et al., 2010b). Aromatic GSLs biosythesis is also composed of three stage such as ‘phenylalanine chain elongation’, ‘core structure formation’, and ‘secondary modification’. Meanwhile, production of indolic GSLs does not have the chain elongation stage (Petersen et al., 2019) (Fig. 1). It is worthy to note that aromatic GSLs biosynthesis pathway has been not clearly defined by studies yet. Genes and enzymes shown in the aromatic GSL pathway in Fig. 1 were characterized in heterologous systems, not in native species (Petersen et al., 2018).

In case of the aliphatic GSLs biosynthesis, amino acid precursor (i.e. methionine) is catalyzed to a corresponding elongated 2-oxo acid by a series of catalytic steps like a deamination step by BRANCHED CHAIN AMINO ACID TRANSFERASE 4 (BCAT4), a condensation step by METHYLTHIOALKYL MALATE SYNTHASES (MAMs), an isomerization step by ISOPROPYLMALATE ISOMERASES (IPMIs), and an oxidative decarboxylation step by ISOPROPYLMALATE DEHYDROGENASES (IPMDHs) in the “chain elongation” stage (Petersen et al., 2019) (Fig. 1). Elongated 2-oxo acid were then transaminated by BRANCHED CHAIN AMINO ACID TRANSFERASE 3 (BCAT3) and subsequently enters into the second stage, “core structure formation”(Halkier and Gershenzon, 2006; Petersen et al., 2018). In case of the aromatic GSL biosynthesis, phenylalanine is used as a precursor, which enter the same catalytic curcuit with the aliphatic GSLs biosynthesis, thus producing homo-phenylalanine (Fig. 1).

The “core structure formation” generates the desulfo-aliphatic GSLs from the corresponding elongated 2-oxo acid (in case of aliphatic GSL pathway) homo-phenylalanine (in case of aromatic GSL pathway) by a seires of catalytic reactions. It is started from the oxidation step by CYTOCHROME P450 MONOOXYGENASE family proteins like CYP79F1, CYP79F2, and CYP83A1, then, a conjugation step by GLUTATHIONE-BY-GLUTATHIONE S-TRANSFERASE F11 (GSTF11) and GLUTATHIONE S-TRANSFERASE

TAU20 (GSTU20). It is further hydrolyzed by GAMMA-GLUTAMYL PEPTIDASE 1 (GGP1), cleaved by C-S LYASE (SUR1), then going through the glycosylation step by UDP-GLUCOSYLTRANSFERASE 74B1 (UGT74B1), and a sulfation step by SULFOTRANSFERASE (SOT17/18) (Halkier and Gershenzon, 2006; Petersen et al., 2018).

At the “secondary modification” stage, a variety of GSLs compounds can be produced by oxidation, alkylation, methoxylation, and desaturation step in Brassicaceae family plants (Rask et al., 2000; Mikkelsen et al., 2002; Grubb and Abel, 2006). For instance, FLAVIN MONOOXYGENASES (FMO GS-OXs) acts to convert methylthioalkyl GSLs to methylsulfinylalkyl GSLs, then methylsulfinylalkyl GSLs is further converted to alkenyl GSLs by ALKENYLHYDROXALKYL-PRODUCING 2 (AOP2) (Hansen et al., 2008). A couple of CYP81F enzymes are responsible for the hydroxylation of indolic GSLs. These hydroxyindolic GSLs can be further methylated by the enzymes like INDOLE GLUCOSINOLATE METHYLTRANSFERASES 1 and 2 (IGMT1 and IGMT1) (Pfalz et al., 2011; Petersen et al., 2018).

As mentioned above, recent studies revealed that vernalization affects not only flowering time of several crops, particularly Brassicaceae family plants but also metabolic changes like glucosinolates (Nugroho et al., 2021; Kang et al., 2022). However, it has been merely explored on the vernalization effect on GSLs biosynthesis in cabbage so far. Thus, we aimed to understand the effect of vernalization on GSLs biosynthesis by integrating RNA-seq and metabolites analyses in this study. This study not only provides insights into vernalization effect on GSLs metabolism in cabbage but also has implications for developing crop varieties that can better adapt to changing environmental conditions.

RESULTS

Profiles of aliphatic, indolic, and aromatic GSLs compounds of cabbage seedlings

For the measurement of glucosinolates (GSLs), cabbage seedlings were grown either in plant culture dishes or in soil. Cabbage seeds were stratified in the dark for 3 days at 4°C to enhance germination, followed by incubation at 22°C under long-day conditions (16 h light/8 h dark). After one week, germinated seedlings were either maintained in plant culture dishes or transferred to soil and further cultivated under the same long-day conditions. The GSL contents and profiles of cabbage seedlings were examined at three non-vernalized time points (NV-14D, NV-54D, and NV-61D) and three vernalized time points (NV-14D, V40, and AV) (Fig. 2A–2B and Supplementary Fig, S2A~S2D). For NV-14D samples, 14-day-old seedlings grown at 22°C under long-day conditions were harvested for HPLC analysis. The NV-54D and NV-61D samples were collected after 54 and 61 days of continuous growth under the same conditions, respectively. For the vernalized (V) time course samples, 14-day-old seedlings were exposed to 4°C for 40 days (V40) after initial growth at 22°C. The after-vernalization (AV) samples were prepared by transferring 40-day-vernalized seedlings back to 22°C and growing them for an additional week before harvest for HPLC analysis.

HPLC analysis of these non-vernalized and vernalized time course samples identified a total of 10 and 11 GSL compounds in plant culture dish and soil-grown samples, respectively (Fig. 2 and Supplementary

Fig. S1 and S2). Among them, six were aliphatic GSLs (progoitrin [PGT], glucoerucin [GER], gluconapin [GNP], glucobrassicanapin [GNA], sinigrin [SIN], and glucoalyssin [GAS]), four were indolic GSLs (4-hydroxyglucobrassicin [4-HGB], glucobrassicin [GBS], 4-methoxyglucobrassicin [4-MTGB], and neoglucobrassicin [NGB]), and one was an aromatic GSL compound (gluconasturtiin [GNT]).

Among six aliphatic GSLs detected in the cabbage seedlings, PGT (progoitrin) was most highly detected and to a lesser extent, SIN and GRA were detected at all tested time points (Fig. 2B-2D, upper panels). It indicated that these three aliphatic GSLs comprise a major portion of total aliphatic GSLs in cabbage. Thus, it is likely that GER-GRA-GNP-PGT production path might be the dominant GSL biosynthetic path in the cabbage seedling (Fig. 1). In case of indolic GSLs, NGB (neoglucobrassicin) and GBS (glucobrassicin) were dominantly detected and to a lesser extent, 4-HGB (4-hydroxyglucobrassicin) and 4-MTGB (4-methoxyglucobrassicin) were detected at all time points (Fig. 2B-2D, lower panels). It indicated that NGB and GBS, these two indolic GSL compounds comprise a high portion of total indolic GSLs in cabbage seedlings. Thus, it seems that GBS-NGB production path might be more dominant than the path spanning GBS-4HGB-4MTGB compounds in cabbage seedling (Fig.1), although we could not detect the intermediate compound, 1OH-I3M in our detection system. In addition, we noticed that amounts of total indolic GSLs were significantly lower that those of total aliphatic GSLs in all three time points regardless of cultivation condition, culture dish or soil (Fig. 2E-2F and Supplementary Fig. S2B~S2D). It indicated that aliphatic GSLs possess a high portion of GSLs in cabbage seedling compared to those of indolic GSLs. In case of aromatic GSL compound, only one compound, GNT was not detected in plant culture dish samples, but very lowly detected in soil-grown samples, thus neglected in further analyses (Fig. 2B~2D and Supplementary Fig. S2B~S2D).

Age-dependent reduction of GSL biosynthesis of cabbage is attenuated by vernalization

In case of plant culture dish samples, Relative amounts of total aliphatic GSLs, indolic GSLs, and total GSLs (combining aliphatic+indolic GSLs) were determined and compared between non-vernalized and vernalized samples along three time points. In case of non-vernalized time course samples, compared to those of NV-14D samples, amounts of total aliphatic GSLs at both NV-54D and NV-61D time points were significantly decreased (Fig. 2F). It indicated that developmental growth of cabbage results in the substantial reduction of total aliphatic GSLs. However, vernalized cabbage samples (V40 and AV) exhibited less reduced amounts of total aliphatic GSLs compared to corresponding non-vernalized samples (NV-54D and NV-61D). It indicated that vernalization might mitigate age-dependent reduction of GSL contents in cabbage.

In case of total indolic GSLs, amount of total indolic GSLs were reduced as plant ages, which was also observed in soil-grown samples (Fig. 2F). However, vernalized samples at V40 and AV time points exhibited rather increased level of indolic GSLs compared to corresponding non-vernalized samples (NV-54D and NV-61D). As a result, while both total aliphatic and indolic GSLs were significantly decreased by developmental growth, vernalization treatment attenuated developmental decline of both aliphatic and

indolic GSLs, thus showing significantly higher amounts of total GSLs in vernalized samples compared to non-vernalized samples (Fig. 2F).

Transcriptome analysis of cabbage seedling along three vernalization time course

Because we observed that vernalization attenuates on developmental decline of aliphatic and indolic GSL metabolism, to dissect transcriptional changes by vernalization, we performed RNA-seq analysis between NV-14D, V40, and AV samples. Three time points of samples, each with three replicates, were prepared. Thus, a total of nine RNA-seq libraries were constructed and sequenced. The result of RNA-seq quality check was presented in Supplementary Table S1. A correlation heatmap of the nine RNA-seq dataset also showed a close clustering of the samples within the same group (Supplementary Fig. S3A), indicating that the RNA-seq libraries were propely constructed along different vernalization time points. Next, we identified differentially expressed genes (DEGs) from three pariwise comparisons among the conditions (Supplementary Fig. S3B). In total, 13,962 genes were differenetially modulated in at least one time point. Among them, the largest number of DEGs was observed in the comparison of V40 compared to AV (10,840 genes), followed by V40 compared to NV (7,801 genes), and AV compared to NV (5,680 genes) (Fig. 3A). In the V40 compared to NV comparison, 3,682 genes were up-regulated and and 4,119 were down-regulated (Fig. 3B). In the AV compared to NV comaparison, 2,038 genes were up-regulated and 3,642 genes were down-regulated. In the V40 compared to AV comparison, 5,753 genes were up-regulated and 5,087 genes were down-regulated.

Gene ontology (GO) analysis using differentially expressed genes in response to vernalization

Because thousand of genes were differentially expressed along vernalization time course (NV, V40, and AV), we conducted to gene ontology (GO) analysis to grasp functional categories significantly affected by vernalization in cabbage. Total 3,682 upregulated and 4,119 downregulated genes in V40 samples in comparison to NV samples were each subjected to GO analysis (Fig. 3C). As a result, functional categories related to chloroplast like ‘photosynthesis’ and ‘linoleic acid metabolisms’ were significantly affected in downregulated genes in V40 samples (Fig. 3C, upper panel). It is in a consistency with previous reports in Brassicaceae family plants including *Arabidopsis thaliana* and *Brassica rapa* (Xi et al. 2020; Dai et al. 2020). In case of upregulated genes in V40 samples, ‘DNA replication’ and ‘glucosinolate biosynthesis’ were significantly detected among top 10 GO terms (Fig. 3C, lower panel). Detection of ‘glucosinolate biosynthesis’ GO term in V40-upregulated genes was in an agreement of our HPLC result (Fig. 2C~2F) showing the attenuated decrease of GSLs in vernalized samples.

In the case of AV samples, a total of 2,038 upregulated and 3,642 downregulated genes were subjected to Gene Ontology (GO) enrichment analysis (Fig. 3D). Even after cabbage seedlings were returned to warm conditions (22 °C, long-day; 16 h light/8 h dark) and grown for seven days, GO terms associated with ‘photosynthesis’ remained among the top-ranked categories identified from downregulated genes (Fig. 3D, upper panel). This suggests that, although the cold treatment had been removed, the plants were still undergoing a gradual physiological adjustment to the new warm environment. For GO terms enriched among upregulated genes in AV samples compared with NV samples, ‘galactose metabolism’

and ‘beta-alanine metabolism’ were significantly represented within the top 10 categories (Fig. 3D, lower panel). The activation of ‘galactose metabolism’ likely reflects enhanced carbohydrate remodeling and the accumulation of protective sugars such as raffinose family oligosaccharides, which might contribute to cold tolerance and energy mobilization during the floral transition. Upregulation of ‘beta-alanine metabolism’–related genes suggests an increased demand for stress-associated metabolites and **coenzyme A (CoA)** intermediates, which are crucial for **fatty acid metabolism** and **energy homeostasis**, supporting metabolic adaptation following cold exposure. Collectively, these results indicate that vernalization induces not only transcriptional reprogramming of flowering-related genes but also broad metabolic adjustments that prime cabbage seedlings for subsequent developmental transitions.

Vernalization induces dynamic transcriptional changes in GSL pathway genes

Because GSLs were significantly shown in Top 10 GO terms using V40-upregulated genes, we further analyzed the transcriptome dataset focusing on GSL pathway genes. For this purpose, we first conducted BLAST searching using 48 *Arabidopsis* GSLs pathway genes and found a total of 78 GSLs pathway genes in cabbage from the *B. oleracea* genome database (Supplementary Table S2). To determine GSL pathway genes that were significantly affected by vernalization, we conducted Venn diagram analysis between 78 *B. oleracea* GSL pathway genes and list of DEGs. Among 78 *B. oleracea* GSL pathway genes, 41 GSL genes were at least one time differentially regulated in paired comparison along three vernalization time points (V40 vs NV, AV vs NV, and V40 vs AV) (Fig. 3E). In more detailed analysis, 3 and 26 GSL genes were respectively detected in the downregulated and upregulated genes in V40 samples compared to NV samples (Fig. 3F). In case of paired comparison between AV and NV, 20 and 4 GSL genes were respectively detected in the downregulated and upregulated genes in AV samples compared to NV samples (Fig. 3G). Collectively, the time-dependent fluctuation of glucosinolate (GSL) pathway genes suggests that GSL metabolism is significantly influenced, showing marked enhancement during vernalization.

Correlation analysis between GSL compounds and transcriptome data along vernalization time course

Heatmap presentation of expression patterns of GSL pathway genes along three vernalization time points (NV, V40, and AV) led us to notice that *B. oleracea* GSL pathway genes can be divided into five different types (Type 1~Type 5) (Fig. 4A and Supplementary Table S4). Each type showed different expression patterns along three vernalization time course. Among these, ‘Type 1’ and ‘Type 3’ exhibited a declining pattern along vernalization, whereas ‘Type 2’, ‘Type 4’, and ‘Type 5’ exhibited increasing pattern either at V40 or AV time points(Fig. 4A). Based on this different pattern, we categorized these types into two groups, VRGs (Vernalization-Repressed GSL genes, total 24 genes combining 21 genes from the ‘Type 1’ and 3 genes from the ‘Type 3’) (Supplementary Table S5) and VIGs (Vernalization-Induced GSL genes, total 46 genes combining 22 genes from the ‘Type 2’, 10 genes from the ‘Type 4’, and 14 genes from the ‘Type 5’) (Supplementary Table S6).

Datasets of the 10 GSL compound profiles (excluding GNT) along vernalization and genes belonging to 24 VRGs or 46 VIGs were combined for the correlation heatmap analysis. First, correlation analysis between 10 GSL compounds and 24 VRGs genes along vernalization were conducted. As a result, 15 GSL pathway genes were detected to be positively correlated with GSL compounds, particularly three GSLs (GRA, SIN, and PGT) of six aliphatic GSLs, which are the most abundant aliphatic GSL compounds (Fig. 4B). These included 6 aliphatic (*BoSOT18d, BoBCAT3b, BoUT74C1b, BoBCAT3a, BoMYB29a*, and *BoMAM1b*), 4 indolic (*BoMYB34, BoCYP79B2a, BoCYP79B2b,* and *BoCYP79B2c*), 4 common genes to aliphatic and indolic (*BoGGP1c, BoAPK2b, BoAPK2c*, and *BoAPK2d*), and 1 aromatic GSL (*BoBZO1a*) genes (Fig, 4C and 4D). To validate the normalized transcirpt profile from RNA-seq dataset, we performed qRT-PCR analysis with selected several genes belonging to 'Type 1' and 'Type3' that showed a high correlation with PGT, GRA, and SIN compound profile. Similar to the results of RNA-seq dataset, we detected expression profiles of the tested genes resembling to the pattern of 'Type 1' and 'Type 3' (Fig. 4E).

Next, we also conducted correlation analysis between the 10 GSL compound profiles and 46 VIG genes along vernalization time course. Resultantly, many VIG group genes (indicated with blue line box) were broadly correlated with 4-MTGB (indolic GSL) profiles along vernalization (Fig. 5A). In addition, we also noticed 15 VIG group genes (indicated with green line box) were significantly correlated with three aliphatic GSL compounds like GNP, GER, GAS, and GBS (indolic GSL) profiles along vernalization. Even three aliphatic GSL compounds, GNP, GER and GAS exhibited higher levels in vernalized (V40 and AV) samples compared to non-vermalized time course samples (NV-54D and NV-61D), their amounts were relatively low among aliphatic GSL compounds (Fig. 5B). Meanwhile, GBS, an indolic GSL compound showing high correlation with 15 VIG group genes were most aboundant among detected four GSL compounds. In addition, amounts of GBS were substantially elevated in vernalized (V40 and AV) samples (indicated with red arrow) in comparison to corresponding non-vernalized (NV-54D and NV-61D) samples (Fig. 5C). Thus, we focused on the 15 VIG group genes which showed a high correlation with GBS profile along vernalization. These 15 VIGs group genes contained two 'Type 4' genes (*BoSOT18a* and *BoSOT16a*) and 13 'Type 5' genes (*BoCYP79F1, BoIPMI_LSU1b, BoSOT18c, BoCYP81F2a, BoIGMT1, BoIGMT2, BoIGMT3, BoIGMT4, BoIGMT5, BoIGMT6, BoIGMT8, BoOBP2*, and *BoAPK1a*) genes (Fig. 5D-5E). To validate the normalized transcirpt profile from RNA-seq dataset, we performed qRT-PCR analysis with selected several genes belonging to 'Type 4' and 'Type5' that showed a high correlation with GBS compound profile. Similar to the results of RNA-seq dataset, we detected expression profiles of the tested genes resembling to the pattern of 'Type 4' and 'Type 5' (Fig. 5F).

Multiple MYB TF genes play crucial role in the regulation of GSL biosynthesis in *Arabidopsis* model plant (Hirai et al., 2007; Sønderby et al., 2007; Gigolashvili et al., 2008). For instance, *MYB28, MYB29*, and *MYB76* are required for regulation of aliphatic GSL biosynthesis, whereas *MYB34, MYB51*, and *MYB122* were reported to play an important role in the control of indolc GSL biosynthesis. Thus, we examined the expression profiles of MYB homologs in *B. oleracea* genome. Total five *B. oleracea* MYB homologs for aliphatic GSL like *BoMYB28a, BoMYB28b, BoMYB28c, BoMYB29a*, and *BoMYB29b* were analyzed for expression profile along vernalization (Fig. 5G). In case of indolic GSL, expression of three *B. oleracea*

MYB homologs like *BoMYB34, BoMYB51,* and *BoMYB122* were presented along vernalization time course (Fig. 5H). Interestingly, six genes (75%) out of total eight *B. oleracea* MYB TF genes, including *BoMYB28a, BoMYB28b, BoMYB28c, BoMYB29b, BoMYB51*, and *BoMYB122* were substantially upregulated during vernalization(Fig. 5G and 5H and Supplementary Fig. S4A-S4B). Upregulation of these *B. oleracea* MYB TFs might also contribute to the enhanced production of aliphatic and indolic GSL compounds in vernalized samples (V40 and AV) compared to corresponding non-vernalized samples (NV-54D and NV-61D).

Based on these observations, we came up with a schematic model illustrating change of aliphatic and indolic GSL profiles along vernalization in cabbage (Fig. 5I). Young cabbage seedlings (2 weeks old) contained high levels of aliphatic (2,384.2 $nmol \cdot g^{-1}$) and indolic GSLs (474.1 $nmol \cdot g^{-1}$). As plants aged, in the absence of vernalization, both aliphatic (797.0 $nmol \cdot g^{-1}$) and indolic GSLs (318.4 $nmol \cdot g^{-1}$) showed a substantial decline. In contrast, vernalization markedly attenuated the reduction of aliphatic GSLs (1,906.6 $nmol \cdot g^{-1}$), and the total amount of indolic GSLs even increased following vernalization (696.5 $nmol \cdot g^{-1}$). It might be at least partily contributed by transcriptional activation of VIG group genes, thus positively influencing production of GSLs. This knowledge could ultimately contribute to the development of cultivation strategies aimed at enhancing GSL accumulation in cabbage, bioactive compounds with anti-cancer and anti-inflammatory properties beneficial to human health. In addition, our transcriptomic dataset provides a valuable foundation for advancing the understanding of developmental and metabolic dynamics associated with vernalization in cabbage.

DISCUSSION

Vernalization triggers transition from vegetative to reproductive stage, and this process is necessary for the optimal flowering of many plants including Brassicaceae family crops. The molecular mechanisms of vernalization, particularly on the floral transition have been extensively studied in *Arabidopsis thaliana*, a dicot model plant belonging to the Brassicaceae family plants (Amasino, 2004; Kim et al., 2009). However, the molecular details underlying metabolic changes in other Brassicaceae family plants by vernalization remains poorly understood. Because GSLs are secondary metabolites produced mainly in Brassicaceae family plants and are involved in the plant defense system against abiotic and biotic stresses (Halkier and Gershenzon, 2006; Bednarek et al., 2009; Clay et al., 2009).

The biosynthesis of GSLs is strongly influenced by environmental cues such as temperature and various abiotic or biotic stresses in Brassicaceae plants (Grubb and Abel, 2006; Yan and Chen, 2007; Hopkins et al., 2009). In this study, we investigated how vernalization affects GSL biosynthesis in cabbage. Transcriptome (RNA-seq) analysis revealed that a substantial portion of GSL biosynthetic genes were transcriptionally reprogrammed in response to vernalization. Notably, many genes involved in the GSL biosynthetic pathway, including *MYB* transcription factors and structural GSL biosynthetic genes, were markedly upregulated following prolonged cold exposure (Fig. 5F–G and Supplementary Fig. S4). Consistent with these transcriptional changes, the reduction in both aliphatic and indolic GSL contents was significantly attenuated by vernalization (Fig. 2E and 2F). In agreement with this observation, our

previous study also demonstrated that vernalization triggers an increase in GSL levels in Chinese cabbage (*Brassica rapa*) (Kang et al., 2022). These results collectively suggest that prolonged cold exposure may induce GSL production in Brassicaceae species, including cabbage. However, in the present study, we examined only the effects of long-term cold treatment (40 days). It remains to be determined whether short-term cold exposure (1–10 days) could exert a similar effect on GSL accumulation. Further studies are therefore needed to clarify the duration and intensity of cold exposure required to attenuate the developmental reduction of GSLs during cabbage growth.

It has been reported that both the quantity and composition of GSLs vary among different tissues and developmental stages. For instance, in Chinese cabbage, outer leaf tissues contain lower levels of GSLs than inner leaf tissues (Rhee et al. 2020; Pucikova et al. 2023). Furthermore, reproductive organs such as flowers and seeds generally accumulate higher levels of GSLs compared with vegetative tissues, including leaves, roots, and stems, in various Brassicaceae species (Feng et al. 2021; Zhang et al. 2023). However, in the case of indolic GSLs, the highest concentrations have been detected in root or shoot tissues in some Brassicaceae plants (Bhandari et al. 2015). This may suggest that different groups of GSLs exhibit distinct biosynthetic responses across various tissues. In addition to tissue specificity, developmental age also dynamically influences GSL accumulation. In case of Chinese cabbage, older plants have been shown to contain substantially lower levels of GSLs compared with young seedlings (Hong and Kim 2014). Considering these previous reports, we tried to minimize potential variability arising from tissue heterogeneity by sampling entire seedlings, rather than selecting specific part of tissues like certain location of leaf for both transcriptomic and metabolomic analyses in this study. To our knowledge, dynamic variations in GSL profiles across tissues, developmental stages, and environmental conditions have not been extensively investigated in cabbage crop plants. Although our study provided an molecular understanding on the effects of vernalization on GSL production in cabbage seedlings, the influence of other environmental factors such as cold, heat, salinity on GSL accumulation remains to be further explored.

In this study, we noticed that GSLs accumulation in cabbage exhibited a marked developmental decline. In the early vegetative stage, two-week-old seedlings contained relatively high levels of total GSLs, whereas their contents drastically decreased by 61 days after germination. This sharp reduction likely reflects a developmental shift in resource allocation from secondary metabolism associated with defense toward primary metabolic processes supporting vegetative growth and reproductive transition. Intriguingly, prolonged cold exposure (40 days), corresponding to vernalization, mitigated this reduction, resulting in a higher glucosinolate content compared with non-vernalized plants of equivalent age. These findings indicate that vernalization not only confers floral competence but also exerts a broader influence on metabolic homeostasis, possibly through the modulation of transcriptional regulators controlling GSLs biosynthetic pathways. Thus, controlled vernalization treatments may represent a feasible strategy to sustain or enhance the accumulation of health-promoting secondary metabolites in *Brassica* crops, particularly within smart-farm or climate-controlled cultivation systems.

MATERIALS AND METHODS

Plant materials and vernalization treatment

Cabbage (*B. oleracea* L. subsp. *capitata*) inbred line 'BN2348' was kindly donated by Asia seed company for RNA-seq and qRT-PCR anlayses. In case of HPLC analysis, due to the limited availability of 'BN2348' inbred cabbage seeds, both 'BN2348' seeds and commercially available *Cabbage* F_1 *'Daebakna'* seeds purchased from Coupang company were used. Seeds were sterilized in 30% bleach solution for 5 min and thoroughly washed several times with sterile distilled water. Sterilized seeds were plated on half-strength Murashige and Skoog (MS) agar media. Non-vernalized seedlings were harvested after the growth for 2 weeks at 22℃ under a long-day photoperiod (16h light: 8h dark), called as non-vernalized (NV) samples. Vernalization treatment was conducted as follows. After the incubation for 2 weeks in growth temperatures at 22℃ under a long-day photoperiod (16h light: 8h dark), seedlings were transferred to the cold refrigerator (4℃) and stored for 40 days under a short-day photoperiod (8h light: 16h dark). After the incubation at 4℃, vernalized seedling plants were incubated for further 7 days at warm temperature 22℃ under a long-day photoperiod (16h light: 8h dark). These vernalized seedlings were called as after-vernalized (AV) samples.

Quantitative real-time PCR (qRT-PCR) analysis

For qRT-PCR analysis, cabbage inbred line 'BN2348' were grown in growth chamber at 22℃ under long day (16h light/8h dark) condition. After growth for 14 days, cabbage seedlings were harvested at ZT4 time point and subjected for total RNA extraction. Total RNAs were extracted using a RNeasy Plant Mini Kit (Qiagen, Germany). DNaseI (NEB, USA) was treated to remove contaminated DNAs. Total 5 μg of total RNAs were subjected to synthesize complementary DNA (cDNA) using EasyScript reverse transcriptase (TransGen Biotech, China). Quantitative RT-PCR (qRT-PCR) reaction was conducted in a LineGene 9600 Plus Real-Time PCR system (BioER, China) using 2X FastFACT™ qPCR Master Mix (BIOFACT, Republic of Korea). A reference gene, *BoPP2Aa* (Bo2g066770) was used for the normalization because it displayed a similar transcript levels along vernalization time course in our normalized RNA-seq dataset. Three biological replicates were prepared and used in the qRT-PCR analysis. Information on the primers used in the qRT-PCR analysis were shown in the Supplementary Table S7.

RNA-seq library construction and sequencing

For RNA-seq analysis, NV, V40, and AV seedling samples were harvested and subjected to the isolation of total RNA using a RNeasy Plant Mini Kit (Qiagen, Germany). Total RNAs were used to build up RNA-seq libraries using a TruSeq Stranded mRNA LT Sample Prep Kit (Illumina Inc., USA) according to the manufacturer's instructions. RNA-seq libraries for three biological replicates per treatment were sequenced on a NovaSeq 6000 system (Insilicogen, South Korea) in the paired-end sequencing method. Quality of the RNA-seq reads was evaluated using the FastQC software. Low quality of reads were trimmed out using the Trimmomatic (ver 0.36) program. Only those with more than 90% threshold (Q > 30) were used for alignment to the *B. oleracea* reference genome downloaded from the BRAD genome database (http://brassicadb.cn/). STAR aligner with default parameters was used for genome alignment

of RNA-seq reads (Dobin et al., 2013). Mapped reads were converted to digital counts using the featureCounts command in R package (Liao et al., 2014). Differentially expressed genes (DEGs) were detected using edgeR (Robinson et al., 2010) based on a 0.05 p-value and a cutoff of a two-fold difference in expression. Venn diagram analyses were performed using a web-based tool (https://www.interactivenn.net/). In addition, mapped reads were converted to bigwig files for the visualization using the Integrative Genomics Viewer (IGV) software developed by the Broad Institute (Thorvaldsdóttir et al., 2013).

Quantification of glucosinolates (GSLs)

Cabbage seedling plants at NV, V40 and AV time points were harvested and then immediately ground in liquid nitrogen. The powders were then incubated with 70% methanol in a water bath at 70 °C for 20 min before cooling. Detailed procedure of GSLs extraction was previously described (Kang et al., 2022). The extracts were dissolved in water (HPLC-grade) and used for desulfo-GSL (DS-GSL) analysis. Separation and quantification of the DS-GSLs were performed on a Vanquish HPLC (Thermo Scientific, USA) with a C18 reverse-phase column (Zorbax XDB-C18, 4.6 × 250 mm, 5 µm particle size, Agilent, USA), using a water and acetonitrile gradient system. All peaks were identified according to the corresponding standard compounds listed in Supplementary Table S8 (Phytoplan, Germany). To quantify the GSLs, DS-sinigrin was used for relative quantification according to ISO91671-1, 1992 (Brown et al., 2003). The contents of individual GSLs were analyzed and shown in nmol/g on a fresh weight basis.

Collection of GSL pathway genes in *B. oleracea* genome

Sequence information of *Arabidopsis* and cabbage homologs was respectively obtained from the TAIR database (http://www.arabidopsis.org) and the Brassicaceae database (BRAD) (http://brassicadb.cn/). Collected amino acid sequence information of 48 GSL pathway genes from Arabidopsis genome were used to retrieve corresponding *B. oleracea* homolog using BLAST search in the BRAD website. Finally, total 78 *B. oleracea* GSL pathway genes were collected and listed in the Supplementary Table S2.

Statistical analysis

One-way analysis of variance (ANOVA) and post-hoc Tukey's test ($p < 0.05$) were used to analyze statistical differences. Data were analyzed using a statistical software package (SAS; version 9.4; SAS Institute Inc., Cary, NC, USA) and presented as the mean ± standard deviation (SD) of three biological replicates.

Declarations

Acknowledgements

Not applicable

Funding

This study was supported by the Korea Forestry Promotion Institute (RS-2025-02213366) and by the National Research Foundation of Korea (grant No. RS-2025-16065991) to D.-H. K. This research was supported by the Chung-Ang University Graduate Research Scholarship in 2024 to EC.

Clinical trial number

Not applicable

Ethics, Consent to Participate, and Consent to Publish declarations

Not applicable

Conflict of interests

The authors declare no conflicts of interest.

Authors contributions

HM and DHK planned this study; HM and EC prepared plant materials and performed the genetic and molecular analyses; HM, MP, and DHK are involved in the bioinformatics analysis; DHK supervised the study and wrote the manuscript

Data availability statement

NGS sequencing data were deposited to the Gene Expression Omnibus database (accession number, GSE229562).

References

1. Amasino, R. (2004). Vernalization, Competence, and the Epigenetic Memory of Winter. *Plant Cell* 16, 2553–2559. doi: 10.1105/TPC.104.161070.
2. Bednarek, P., Piślewska-Bednarek, M., Svatoš, A., Schneider, B., Doubský, J., Mansurova, M., et al. (2009). A glucosinolate metabolism pathway in living plant cells mediates broad-spectrum antifungal defense. *Science (80-.).* 323, 101–106. doi: 10.1126/SCIENCE.1163732/SUPPL_FILE/BEDNAREK.SOM.PDF.
3. Bell, L., Oloyede, O. O., Lignou, S., Wagstaff, C., and Methven, L. (2018). Taste and Flavor Perceptions of Glucosinolates, Isothiocyanates, and Related Compounds. *Mol. Nutr. Food Res.* 62, 1700990. doi: 10.1002/MNFR.201700990.
4. Brown, P. D., Tokuhisa, J. G., Reichelt, M., and Gershenzon, J. (2003). Variation of glucosinolate accumulation among different organs and developmental stages of Arabidopsis thaliana. *Phytochemistry* 62, 471–481. doi: 10.1016/S0031-9422(02)00549-6.
5. Celenza, J. L., Quiel, J. A., Smolen, G. A., Merrikh, H., Silvestro, A. R., Normanly, J., et al. (2005). The arabidopsis ATR1 Myb transcription factor controls indolic glucosinolate homeostasis. *Plant*

Physiol. 137, 253–262. doi: 10.1104/pp.104.054395.

6. Clay, N. K., Adio, A. M., Denoux, C., Jander, G., and Ausubel, F. M. (2009). Glucosinolate metabolites required for an Arabidopsis innate immune response. *Science (80-.).* 323, 95–101. doi: 10.1126/SCIENCE.1164627/SUPPL_FILE/CLAY.SOM.REV.PDF.
7. Corpet, F. (1988). Multiple sequence alignment with hierarchical clustering. *Nucleic Acids Res.* 16, 10881–10890. doi: 10.1093/NAR/16.22.10881.
8. Czechowski, T., Stitt, M., Altmann, T., Udvardi, M. K., and Scheible, W. R. (2005). Genome-Wide Identification and Testing of Superior Reference Genes for Transcript Normalization in Arabidopsis. *Plant Physiol.* 139, 5–17. doi: 10.1104/PP.105.063743.
9. Dobin, A., Davis, C. A., Schlesinger, F., Drenkow, J., Zaleski, C., Jha, S., et al. (2013). STAR: ultrafast universal RNA-seq aligner. *Bioinformatics* 29, 15–21. doi: 10.1093/BIOINFORMATICS/BTS635.
10. Fahey, J. W., Zalcmann, A. T., and Talalay, P. (2001). The chemical diversity and distribution of glucosinolates and isothiocyanates among plants. *Phytochemistry* 56, 5–51. doi: 10.1016/S0031-9422(00)00316-2.
11. Gigolashvili, T., Berger, B., Mock, H. P., Müller, C., Weisshaar, B., and Flügge, U. I. (2007). The transcription factor HIG1/MYB51 regulates indolic glucosinolate biosynthesis in Arabidopsis thaliana. *Plant J.* 50, 886–901. doi: 10.1111/j.1365-313X.2007.03099.x.
12. Gigolashvili, T., Engqvist, M., Yatusevich, R., Müller, C., and Flügge, U. I. (2008). HAG2/MYB76 and HAG3/MYB29 exert a specific and coordinated control on the regulation of aliphatic glucosinolate biosynthesis in Arabidopsis thaliana. *New Phytol.* 177, 627–642. doi: 10.1111/j.1469-8137.2007.02295.x.
13. Grubb, C. D., and Abel, S. (2006). Glucosinolate metabolism and its control. *Trends Plant Sci.* 11, 89–100. doi: 10.1016/J.TPLANTS.2005.12.006.
14. Halkier, B. A., and Gershenzon, J. (2006). Biology and biochemistry of glucosinolates. *Annu. Rev. Plant Biol.* 57, 303–333. doi: 10.1146/annurev.arplant.57.032905.105228.
15. Hansen, B. G., Kerwin, R. E., Ober, J. A., Lambrix, V. M., Mitchell-Olds, T., Gershenzon, J., et al. (2008). A novel 2-oxoacid-dependent dioxygenase involved in the formation of the goiterogenic 2-hydroxybut-3-enyl glucosinolate and generalist insect resistance in Arabidopsis. *Plant Physiol.* 148, 2096–2108. doi: 10.1104/pp.108.129981.
16. Hirai, M. Y., Sugiyama, K., Sawada, Y., Tohge, T., Obayashi, T., Suzuki, A., et al. (2007). Omics-based identification of Arabidopsis Myb transcription factors regulating aliphatic glucosinolate biosynthesis. *Proc. Natl. Acad. Sci. U. S. A.* 104, 6478–6483. doi: 10.1073/pnas.0611629104.
17. Hopkins, R. J., Van Dam, N. M., and Van Loon, J. J. A. (2009). Role of glucosinolates in insect-plant relationships and multitrophic interactions. *Annu. Rev. Entomol.* 54, 57–83. doi: 10.1146/annurev.ento.54.110807.090623.
18. Kang, H., Nugroho, A. B. D., Park, M., Kim, J. A., Lee, S. W., Moon, H., et al. (2022). Vernalization Regulates Flowering Genes and Modulates Glucosinolates Biosynthesis in Chinese Cabbage. *J. Plant Biol.* 65, 157–173. doi: 10.1007/S12374-021-09344-Z/METRICS.

19. Keck, A. S., and Finley, J. W. (2004). Cruciferous Vegetables: Cancer Protective Mechanisms of Glucosinolate Hydrolysis Products and Selenium. *Integr. Cancer Ther.* 3, 5–12. doi: 10.1177/1534735403261831.
20. Kim, D. H., Doyle, M. R., Sung, S., and Amasino, R. M. (2009). Vernalization: Winter and the timing of flowering in plants. *Annu. Rev. Cell Dev. Biol.* 25, 277–299. doi: 10.1146/ANNUREV.CELLBIO.042308.113411/CITE/REFWORKS.
21. Kim D.H., Sung S.. (2017). The Binding Specificity of the PHD-Finger Domain of VIN3 Moderates Vernalization Response. Plant Physiol. 173(2), 1258-1268. doi: 10.1104/pp.16.01320.
22. Bhandari SR, Jo JS, Lee JG (2015) Comparison of Glucosinolate Profiles in Different Tissues of Nine Brassica Crops. Molecules 20 (9):15827–15841. doi:10.3390/molecules200915827
23. Dai Y, Zhang S, Sun X, Li G, Yuan L, Li F, Zhang H, Zhang S, Chen G, Wang C, Sun R (2020) Comparative Transcriptome Analysis of Gene Expression and Regulatory Characteristics Associated with Different Vernalization Periods in Brassica rapa. Genes (Basel) 11 (4). doi:10.3390/genes11040392
24. Feng X, Ma J, Liu Z, Li X, Wu Y, Hou L, Li M (2021) Analysis of Glucosinolate Content and Metabolism Related Genes in Different Parts of Chinese Flowering Cabbage. Front Plant Sci 12:767898. doi:10.3389/fpls.2021.767898
25. Hong E, Kim GH (2014) Variation of Glucosinolate Composition during Seedling and Growth Stages of
26. L. ssp. Korean J Hortic Sci 32 (5):730–738. doi:10.7235/hort.2014.14041
27. Pucikova V, Rohn S, Hanschen FS (2023) Glucosinolate Accumulation and Hydrolysis in Leafy Brassica Vegetables Are Influenced by Leaf Age. J Agric Food Chem 71 (30):11466–11475. doi:10.1021/acs.jafc.3c01997
28. Rhee JH, Choi S, Lee JE, Hur OS, Ro NY, Hwang AJ, Ko HC, Chung YJ, Noh JJ, Assefa AD (2020) Glucosinolate Content in Brassica Genetic Resources and Their Distribution Pattern within and between Inner, Middle, and Outer Leaves. Plants (Basel) 9 (11). doi:10.3390/plants9111421
29. Xi Y, Park SR, Kim DH, Kim ED, Sung S (2020) Transcriptome and epigenome analyses of vernalization in Arabidopsis thaliana. Plant J 103 (4):1490–1502. doi:10.1111/tpj.14817
30. Zhang R, Zhang J, Li C, Pan Q, Haq SU, Mosa WFA, Fang F, Zhang L, Li B (2023) The Accumulation of Health-Promoting Nutrients from Representative Organs across Multiple Developmental Stages in Orange Chinese Cabbage. Plants (Basel) 12 (11). doi:10.3390/plants12112120
31. Bhandari SR, Jo JS, Lee JG (2015) Comparison of Glucosinolate Profiles in Different Tissues of Nine Brassica Crops. Molecules 20 (9):15827–15841. doi:10.3390/molecules200915827
32. Dai Y, Zhang S, Sun X, Li G, Yuan L, Li F, Zhang H, Zhang S, Chen G, Wang C, Sun R (2020) Comparative Transcriptome Analysis of Gene Expression and Regulatory Characteristics Associated with Different Vernalization Periods in Brassica rapa. Genes (Basel) 11 (4). doi:10.3390/genes11040392

33. Feng X, Ma J, Liu Z, Li X, Wu Y, Hou L, Li M (2021) Analysis of Glucosinolate Content and Metabolism Related Genes in Different Parts of Chinese Flowering Cabbage. Front Plant Sci 12:767898. doi:10.3389/fpls.2021.767898
34. Hong E, Kim GH (2014) Variation of Glucosinolate Composition during Seedling and Growth Stages of
35. L. ssp. Korean J Hortic Sci 32 (5):730–738. doi:10.7235/hort.2014.14041
36. Pucikova V, Rohn S, Hanschen FS (2023) Glucosinolate Accumulation and Hydrolysis in Leafy Brassica Vegetables Are Influenced by Leaf Age. J Agric Food Chem 71 (30):11466–11475. doi:10.1021/acs.jafc.3c01997
37. Rhee JH, Choi S, Lee JE, Hur OS, Ro NY, Hwang AJ, Ko HC, Chung YJ, Noh JJ, Assefa AD (2020) Glucosinolate Content in Brassica Genetic Resources and Their Distribution Pattern within and between Inner, Middle, and Outer Leaves. Plants (Basel) 9 (11). doi:10.3390/plants9111421
38. Xi Y, Park SR, Kim DH, Kim ED, Sung S (2020) Transcriptome and epigenome analyses of vernalization in Arabidopsis thaliana. Plant J 103 (4):1490–1502. doi:10.1111/tpj.14817
39. Zhang R, Zhang J, Li C, Pan Q, Haq SU, Mosa WFA, Fang F, Zhang L, Li B (2023) The Accumulation of Health-Promoting Nutrients from Representative Organs across Multiple Developmental Stages in Orange Chinese Cabbage. Plants (Basel) 12 (11). doi:10.3390/plants12112120
40. Bhandari SR, Jo JS, Lee JG (2015) Comparison of Glucosinolate Profiles in Different Tissues of Nine Brassica Crops. Molecules 20 (9):15827–15841. doi:10.3390/molecules200915827
41. Dai Y, Zhang S, Sun X, Li G, Yuan L, Li F, Zhang H, Zhang S, Chen G, Wang C, Sun R (2020) Comparative Transcriptome Analysis of Gene Expression and Regulatory Characteristics Associated with Different Vernalization Periods in Brassica rapa. Genes (Basel) 11 (4). doi:10.3390/genes11040392
42. Feng X, Ma J, Liu Z, Li X, Wu Y, Hou L, Li M (2021) Analysis of Glucosinolate Content and Metabolism Related Genes in Different Parts of Chinese Flowering Cabbage. Front Plant Sci 12:767898. doi:10.3389/fpls.2021.767898
43. Hong E, Kim GH (2014) Variation of Glucosinolate Composition during Seedling and Growth Stages of
44. L. ssp. Korean J Hortic Sci 32 (5):730–738. doi:10.7235/hort.2014.14041
45. Pucikova V, Rohn S, Hanschen FS (2023) Glucosinolate Accumulation and Hydrolysis in Leafy Brassica Vegetables Are Influenced by Leaf Age. J Agric Food Chem 71 (30):11466–11475. doi:10.1021/acs.jafc.3c01997
46. Rhee JH, Choi S, Lee JE, Hur OS, Ro NY, Hwang AJ, Ko HC, Chung YJ, Noh JJ, Assefa AD (2020) Glucosinolate Content in Brassica Genetic Resources and Their Distribution Pattern within and between Inner, Middle, and Outer Leaves. Plants (Basel) 9 (11). doi:10.3390/plants9111421
47. Xi Y, Park SR, Kim DH, Kim ED, Sung S (2020) Transcriptome and epigenome analyses of vernalization in Arabidopsis thaliana. Plant J 103 (4):1490–1502. doi:10.1111/tpj.14817

48. Zhang R, Zhang J, Li C, Pan Q, Haq SU, Mosa WFA, Fang F, Zhang L, Li B (2023) The Accumulation of Health-Promoting Nutrients from Representative Organs across Multiple Developmental Stages in Orange Chinese Cabbage. Plants (Basel) 12 (11). doi:10.3390/plants12112120
49. Bhandari SR, Jo JS, Lee JG (2015) Comparison of Glucosinolate Profiles in Different Tissues of Nine Brassica Crops. Molecules 20 (9):15827–15841. doi:10.3390/molecules200915827
50. Feng X, Ma J, Liu Z, Li X, Wu Y, Hou L, Li M (2021) Analysis of Glucosinolate Content and Metabolism Related Genes in Different Parts of Chinese Flowering Cabbage. Front Plant Sci 12:767898. doi:10.3389/fpls.2021.767898
51. Hong E, Kim GH (2014) Variation of Glucosinolate Composition during Seedling and Growth Stages of
52. L. ssp. Korean J Hortic Sci 32 (5):730–738. doi:10.7235/hort.2014.14041
53. Pucikova V, Rohn S, Hanschen FS (2023) Glucosinolate Accumulation and Hydrolysis in Leafy Brassica Vegetables Are Influenced by Leaf Age. J Agric Food Chem 71 (30):11466–11475. doi:10.1021/acs.jafc.3c01997
54. Rhee JH, Choi S, Lee JE, Hur OS, Ro NY, Hwang AJ, Ko HC, Chung YJ, Noh JJ, Assefa AD (2020) Glucosinolate Content in Brassica Genetic Resources and Their Distribution Pattern within and between Inner, Middle, and Outer Leaves. Plants (Basel) 9 (11). doi:10.3390/plants9111421
55. Xi Y, Park SR, Kim DH, Kim ED, Sung S (2020) Transcriptome and epigenome analyses of vernalization in Arabidopsis thaliana. Plant J 103 (4):1490–1502. doi:10.1111/tpj.14817
56. Zhang R, Zhang J, Li C, Pan Q, Haq SU, Mosa WFA, Fang F, Zhang L, Li B (2023) The Accumulation of Health-Promoting Nutrients from Representative Organs across Multiple Developmental Stages in Orange Chinese Cabbage. Plants (Basel) 12 (11). doi:10.3390/plants12112120
57. Bhandari SR, Jo JS, Lee JG (2015) Comparison of Glucosinolate Profiles in Different Tissues of Nine Brassica Crops. Molecules 20 (9):15827–15841. doi:10.3390/molecules200915827
58. Feng X, Ma J, Liu Z, Li X, Wu Y, Hou L, Li M (2021) Analysis of Glucosinolate Content and Metabolism Related Genes in Different Parts of Chinese Flowering Cabbage. Front Plant Sci 12:767898. doi:10.3389/fpls.2021.767898
59. Pucikova V, Rohn S, Hanschen FS (2023) Glucosinolate Accumulation and Hydrolysis in Leafy Brassica Vegetables Are Influenced by Leaf Age. J Agric Food Chem 71 (30):11466–11475. doi:10.1021/acs.jafc.3c01997
60. Rhee JH, Choi S, Lee JE, Hur OS, Ro NY, Hwang AJ, Ko HC, Chung YJ, Noh JJ, Assefa AD (2020) Glucosinolate Content in Brassica Genetic Resources and Their Distribution Pattern within and between Inner, Middle, and Outer Leaves. Plants (Basel) 9 (11). doi:10.3390/plants9111421
61. Xi Y, Park SR, Kim DH, Kim ED, Sung S (2020) Transcriptome and epigenome analyses of vernalization in Arabidopsis thaliana. Plant J 103 (4):1490–1502. doi:10.1111/tpj.14817
62. Zhang R, Zhang J, Li C, Pan Q, Haq SU, Mosa WFA, Fang F, Zhang L, Li B (2023) The Accumulation of Health-Promoting Nutrients from Representative Organs across Multiple Developmental Stages in Orange Chinese Cabbage. Plants (Basel) 12 (11). doi:10.3390/plants12112120

63. Feng X, Ma J, Liu Z, Li X, Wu Y, Hou L, Li M (2021) Analysis of Glucosinolate Content and Metabolism Related Genes in Different Parts of Chinese Flowering Cabbage. Front Plant Sci 12:767898. doi:10.3389/fpls.2021.767898
64. Pucikova V, Rohn S, Hanschen FS (2023) Glucosinolate Accumulation and Hydrolysis in Leafy Brassica Vegetables Are Influenced by Leaf Age. J Agric Food Chem 71 (30):11466–11475. doi:10.1021/acs.jafc.3c01997
65. Rhee JH, Choi S, Lee JE, Hur OS, Ro NY, Hwang AJ, Ko HC, Chung YJ, Noh JJ, Assefa AD (2020) Glucosinolate Content in Brassica Genetic Resources and Their Distribution Pattern within and between Inner, Middle, and Outer Leaves. Plants (Basel) 9 (11). doi:10.3390/plants9111421
66. Xi Y, Park SR, Kim DH, Kim ED, Sung S (2020) Transcriptome and epigenome analyses of vernalization in Arabidopsis thaliana. Plant J 103 (4):1490–1502. doi:10.1111/tpj.14817
67. Zhang R, Zhang J, Li C, Pan Q, Haq SU, Mosa WFA, Fang F, Zhang L, Li B (2023) The Accumulation of Health-Promoting Nutrients from Representative Organs across Multiple Developmental Stages in Orange Chinese Cabbage. Plants (Basel) 12 (11). doi:10.3390/plants12112120
68. Feng X, Ma J, Liu Z, Li X, Wu Y, Hou L, Li M (2021) Analysis of Glucosinolate Content and Metabolism Related Genes in Different Parts of Chinese Flowering Cabbage. Front Plant Sci 12:767898. doi:10.3389/fpls.2021.767898
69. Pucikova V, Rohn S, Hanschen FS (2023) Glucosinolate Accumulation and Hydrolysis in Leafy Brassica Vegetables Are Influenced by Leaf Age. J Agric Food Chem 71 (30):11466–11475. doi:10.1021/acs.jafc.3c01997
70. Rhee JH, Choi S, Lee JE, Hur OS, Ro NY, Hwang AJ, Ko HC, Chung YJ, Noh JJ, Assefa AD (2020) Glucosinolate Content in Brassica Genetic Resources and Their Distribution Pattern within and between Inner, Middle, and Outer Leaves. Plants (Basel) 9 (11). doi:10.3390/plants9111421
71. Xi Y, Park SR, Kim DH, Kim ED, Sung S (2020) Transcriptome and epigenome analyses of vernalization in Arabidopsis thaliana. Plant J 103 (4):1490–1502. doi:10.1111/tpj.14817
72. Pucikova V, Rohn S, Hanschen FS (2023) Glucosinolate Accumulation and Hydrolysis in Leafy Brassica Vegetables Are Influenced by Leaf Age. J Agric Food Chem 71 (30):11466–11475. doi:10.1021/acs.jafc.3c01997
73. Rhee JH, Choi S, Lee JE, Hur OS, Ro NY, Hwang AJ, Ko HC, Chung YJ, Noh JJ, Assefa AD (2020) Glucosinolate Content in Brassica Genetic Resources and Their Distribution Pattern within and between Inner, Middle, and Outer Leaves. Plants (Basel) 9 (11). doi:10.3390/plants9111421
74. Xi Y, Park SR, Kim DH, Kim ED, Sung S (2020) Transcriptome and epigenome analyses of vernalization in Arabidopsis thaliana. Plant J 103 (4):1490–1502. doi:10.1111/tpj.14817
75. Rhee JH, Choi S, Lee JE, Hur OS, Ro NY, Hwang AJ, Ko HC, Chung YJ, Noh JJ, Assefa AD (2020) Glucosinolate Content in Brassica Genetic Resources and Their Distribution Pattern within and between Inner, Middle, and Outer Leaves. Plants (Basel) 9 (11). doi:10.3390/plants9111421
76. Xi Y, Park SR, Kim DH, Kim ED, Sung S (2020) Transcriptome and epigenome analyses of vernalization in Arabidopsis thaliana. Plant J 103 (4):1490–1502. doi:10.1111/tpj.14817

77. Xi Y, Park SR, Kim DH, Kim ED, Sung S (2020) Transcriptome and epigenome analyses of vernalization in Arabidopsis thaliana. Plant J 103 (4):1490–1502. doi:10.1111/tpj.14817
78. Liao, Y., Smyth, G. K., and Shi, W. (2014). FeatureCounts: An efficient general purpose program for assigning sequence reads to genomic features. *Bioinformatics* 30, 923–930. doi: 10.1093/BIOINFORMATICS/BTT656.
79. Malitsky, S., Blum, E., Less, H., Venger, I., Elbaz, M., Morin, S., et al. (2008). The transcript and metabolite networks affected by the two clades of Arabidopsis glucosinolate biosynthesis regulators. *Plant Physiol.* 148, 2021–2049. doi: 10.1104/pp.108.124784.
80. Mi ekus, N., Marszałek, K., Podlacha, M., Iqbal, A., Puchalski, C., and Swiergiel, A. H. (2020). Health Benefits of Plant-Derived Sulfur Compounds, Glucosinolates, and Organosulfur Compounds. *Mol. 2020, Vol. 25, Page 3804* 25, 3804. doi: 10.3390/MOLECULES25173804.
81. Mikkelsen, M. D., Petersen, B. L., Olsen, C. E., and Halkier, B. A. (2002). Biosynthesis and metabolic engineering of glucosinolates. *Amino Acids* 22, 279–295. doi: 10.1007/S007260200014/METRICS.
82. Moon, H., Hwang, B. H., Park, M., Huq, E., and Kim, D. H. (2024). Time Course Transcriptomic Analysis of Cabbage (Brassica oleracea ssp. capitata L.) During Vernalization. *J. Plant Biol.* 67, 317–332. doi: 10.1007/S12374-024-09430-Y/METRICS.
83. Nugroho, A. B. D., Lee, S. W., Pervitasari, A. N., Moon, H., Choi, D., Kim, J., et al. (2021). Transcriptomic and metabolic analyses revealed the modulatory effect of vernalization on glucosinolate metabolism in radish (Raphanus sativus L.). *Sci. Reports 2021 111* 11, 1–15. doi: 10.1038/s41598-021-03557-5.
84. Petersen, A., Hansen, L. G., Mirza, N., Crocoll, C., Mirza, O., and Halkier, B. A. (2019). Changing substrate specificity and iteration of amino acid chain elongation in glucosinolate biosynthesis through targeted mutagenesis of Arabidopsis methylthioalkylmalate synthase 1. *Biosci. Rep.* 39. doi: 10.1042/BSR20190446/219297.
85. Petersen, A., Wang, C., Crocoll, C., and Halkier, B. A. (2018). Biotechnological approaches in glucosinolate production. *J. Integr. Plant Biol.* 60, 1231–1248. doi: 10.1111/JIPB.12705.
86. Pfalz, M., Mikkelsen, M. D., Bednarek, P., Olsen, C. E., Halkier, B. A., and Kroymann, J. (2011). Metabolic Engineering in Nicotiana benthamiana Reveals Key Enzyme Functions in Arabidopsis Indole Glucosinolate Modification. *Plant Cell* 23, 716–729. doi: 10.1105/TPC.110.081711.
87. Rask, L., Andréasson, E., Ekbom, B., Eriksson, S., Pontoppidan, B., and Meijer, J. (2000). Myrosinase: Gene family evolution and herbivore defense in Brassicaceae. *Plant Mol. Biol.* 42, 93–114. doi: 10.1023/A:1006380021658.
88. Robinson, M. D., McCarthy, D. J., and Smyth, G. K. (2010). edgeR: a Bioconductor package for differential expression analysis of digital gene expression data. *Bioinformatics* 26, 139–140. doi: 10.1093/BIOINFORMATICS/BTP616.
89. Schuettengruber B, Chourrout D, Vervoort M, Leblanc B, Cavalli G. (2007) Genome regulation by polycomb and trithorax proteins. *Cell* 128(4), 735-45. doi: 10.1016/j.cell.2007.02.009. PMID: 17320510.

90. Sønderby, I. E., Burow, M., Rowe, H. C., Kliebenstein, D. J., and Halkier, B. A. (2010a). A Complex Interplay of Three R2R3 MYB Transcription Factors Determines the Profile of Aliphatic Glucosinolates in Arabidopsis. *Plant Physiol.* 153, 348–363. doi: 10.1104/PP.109.149286.
91. Sønderby, I. E., Geu-Flores, F., and Halkier, B. A. (2010b). Biosynthesis of glucosinolates - gene discovery and beyond. *Trends Plant Sci.* 15, 283–290. doi: 10.1016/j.tplants.2010.02.005.
92. Sønderby, I. E., Hansen, B. G., Bjarnholt, N., Ticconi, C., Halkier, B. A., and Kliebenstein, D. J. (2007). A Systems Biology Approach Identifies a R2R3 MYB Gene Subfamily with Distinct and Overlapping Functions in Regulation of Aliphatic Glucosinolates. *PLoS One* 2, e1322. doi: 10.1371/JOURNAL.PONE.0001322.
93. Steindal, A. L. H., Rdven, R., Hansen, E., and Mlmann, J. (2015). Effects of photoperiod, growth temperature and cold acclimatisation on glucosinolates, sugars and fatty acids in kale. *Food Chem.* 174, 44–51. doi: 10.1016/J.FOODCHEM.2014.10.129.
94. Thorvaldsdóttir, H., Robinson, J. T., and Mesirov, J. P. (2013). Integrative Genomics Viewer (IGV): High-performance genomics data visualization and exploration. *Brief. Bioinform.* 14, 178–192. doi: 10.1093/BIB/BBS017.
95. Verhoeven, D. T. H., Goldbohm, R. A., Van Poppel, G., Verhagen, H., and Van Den Brandt, P. A. (1996). Epidemiological studies on Brassica vegetables and cancer risk. *Cancer Epidemiol. Biomarkers Prev.* 5, 733–748.
96. Yan, X., and Chen, S. (2007). Regulation of plant glucosinolate metabolism. *Planta* 226, 1343–1352. doi: 10.1007/S00425-007-0627-7/METRICS.

Figures

Figure 1.

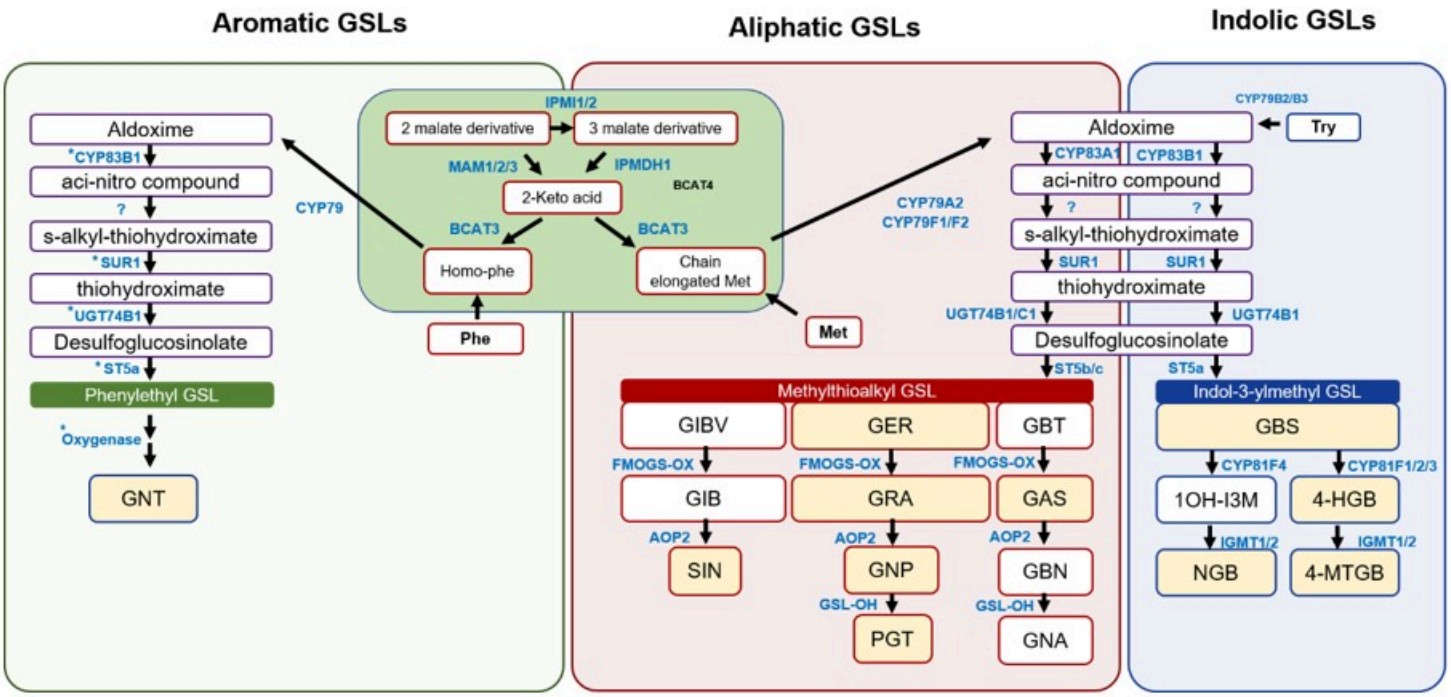

Figure 1

Schematic pathways of aliphatic, indolic and aromatic GSLs biosynthesis in the Brassicaceae family plants. The ‘side-chain elongation’ process is represented within the green box located between aromatic and aliphatic GSL pathway, which is common to the aliphatic and aromatic GSL pathway. White box indicates the individual compound catalyzed by metabolic enzymes (indicated with blue letters) in each step. Total 11 GSL compounds were detected in this study and presented with yellow boxes, whereas undetected GSLs are indicated with white color boxes. Arrows represent direction of pathways for aliphatic, indolic, and aromatic GSLs biosynthesis, respectively. Asterisk (*) Indicates that those genes and/or enzymes were characterized in heterologous systems, not in native species. Progoitrin (PGT); Glucoraphanin (GRA); Sinigrin (SIN); Glucoalyssin (GAS); Gluconapin (GNP); 4-Hydroxyglucobrassicin (4-HGB); Glucoerucin (GER); Glucobrassicin (GBS); 4-Methoxyglucobrassicin (4-MTGB); Gluconasturtiin (GNT); Neoglucobrassicin (NGB).

Figure 2.

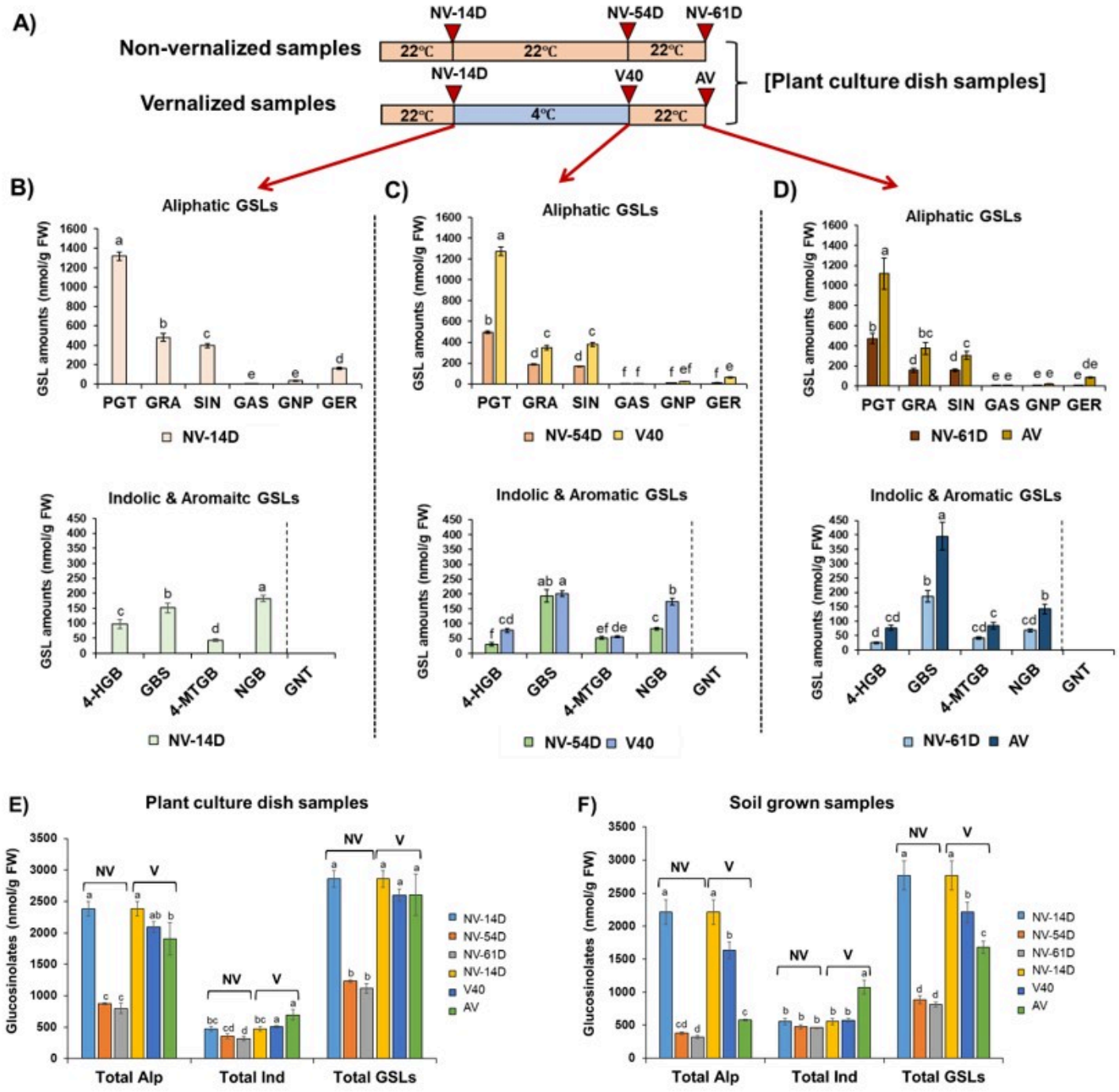

Figure 2

Quantification of aliphatic and indolic GSL compounds of cabbage in non-vernalized three time course (NV-14 days, NV-54 days, and NV-61 days) or vernalized three time course (NV-14 days, V40, and AV). A) a diagram showing sampling time points for non-vernalized three time points (NV-14 days, NV-54 days, and NV-61 days) and vernalized three time points (NV-14 days, V40, and AV) used for HPLC analysis. Each time point for sampling was indicated with red downward arrowhead. Amounts of six different aliphatic GSL compounds along three vernalization time points (NV, non-vernalized; V40, 40 days-

vernalized; AV, after-vernalized). NV-14D: non-vernalized cabbage seedlings grown for 14 days; NV-54D: non-vernalized cabbage seedlings grown for 54 days; NV-61D: non-vernalized cabbage seedlings grown for 61 days. Non-vernalized seedlings were continuously grown in plant culture dish under long day (16h light: 8h dark) condition. V40: 2-week-old seedlings were transferred to cold (4℃) and incubated for 40 days under short-day (8h light: 16 dark) condition; AV: Vernalized cabbage seedlings at 4℃ for 40 days were returned to warm (22℃) temperature for further growth for 7 days. **B)**Quantification of six aliphatic GSLs (upper panel) and four indolic GSLs and one aromatic GSL compound (lower panel) of 2-week cabbage seedling samples (NV-14D) **C)** Quantification of six aliphatic GSLs (upper panel) and four indolic GSLs and one aromatic GSL compound (lower panel) of non-vernalized NV-54D samples and corresponding vernalized V40 samples. **D)** Quantification of six aliphatic GSLs (upper panel) and four indolic GSLs and one aromatic GSL compound (lower panel) of non-vernalized NV-61D samples and corresponding vernalized AV samples. **E)** Comparison of total aliphatic GSLs, indolic GSLs , and total GSLs (combinding amounts of total aliphatic and indolic GSLs) contents of cabbage seedling grown in plant culture dish during three non-vernalized time course (NV-14D, non-vernalized cabbage seedlings grown for 14 days; NV-54D, non-vernalized cabbage seedlings continuously grown for 54 days in warm (22℃) temperature; NV-61D, non-vernalized cabbage seedlings continuously grown for 61 days in warm (22℃) temperature) and three vernalized time course (NV-14D, non-vernalized cabbage seedling grown for 14 days; V40, vernalized cabbage seedlings for 40 days at 4℃; AV, cabbage seedlings exposed to 40 days of cold, and then further grown for 7 days in warm (22℃) temperature. NV: non-vernalized, V: vernalized. **F)** Comparison of total aliphatic GSLs, indolic GSLs , and total GSLs (combinding amounts of total aliphatic and indolic GSLs) contents of cabbage seedling grown in soil during three non-vernalized time course (NV-14D, non-vernalized cabbage seedlings grown in petri dish for 7 days and then transferred to soil for another 7 day-growth; NV-54D, non-vernalized cabbage seedlings continuously grown in soil for 54 days in warm (22℃) temperature; NV-61D, non-vernalized cabbage seedlings continuously grown in soil for 61 days in warm (22℃) temperature) and three vernalized time course (NV-14D, non-vernalized cabbage seedling grown for 14 days; V40, vernalized cabbage seedlings for 40 days at 4℃; AV, cabbage seedlings exposed to 40 days of cold, and then further grown for 7 days in warm (22℃) temperature. NV: non-vernalized, V: vernalized. **B)~D)**One aromatic GSL compound was not detected in our HPLC detection system used for plant culture dish samples. **B)~F)**Data were presented as mean ± standard deviation (SD) (n=3). Statistically significant differences were determined by one-way ANOVA and Tukey's post hoc test ($p < 0.05$).

Figure 3.

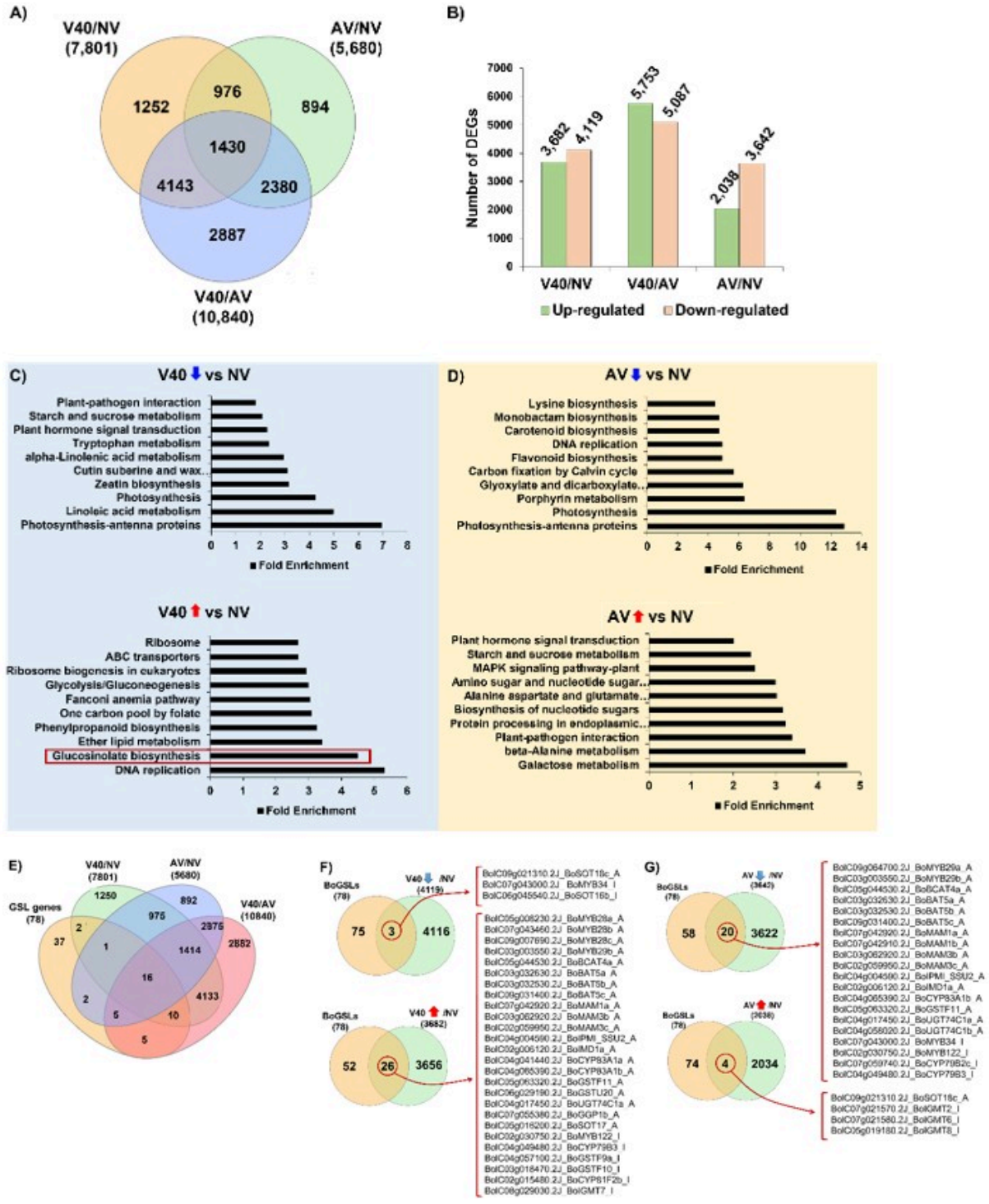

Figure 3

Identification of differentially expressed genes (DEGs) by pair-wise comparison among three vernalization time course (NV, V40, and AV). A) A Venn diagram showing the number of differentially expressed genes (DEGs) that are unique to or shared among the three pairwise comparisons across the vernalization time course. **B)** The number of up-regulated and down-regulated genes identified from three pariwise comparisons among three vernalization time points. **C)** Result of gene ontology (GO)

analysis using upregulated genes in V40 samples compared to NV samples (upper panel) and downregulated genes in V40 samples compared to NV samples (lower panel). Top 10 ranked GO categories were presented based on the fold enrichment score using ShinyGO web-based tool (ver0.81) (https://bioinformatics.sdstate.edu/go81/). **D)** Result of gene ontology (GO) analysis using upregulated genes in AV samples compared to NV samples (upper panel) and downregulated genes in AV samples compared to NV samples (lower panel). Top 10 ranked GO categories were presented based on the fold enrichment score using ShinyGO web-based tool (ver0.81) (https://bioinformatics.sdstate.edu/go81/). **E)** Result of Venn diagram analysis with 78 *B. oleracea* GSL pathway genes and list of differentially expressed genes (DEGs) obtained from three pairwise comparisons (V40 vs NV, AV vs NV, and V40 vs AV) across the vernalization time course. **F)** Venn diagram analysis showing the overlap between 78 *B. oleracea* GSL pathway genes and differentially expressed genes (DEGs) in V40 samples compared with NV samples. The upper panel shows three GSL pathway genes that were downregulated among 4,119 DEGs, while the lower panel shows 26 GSL pathway genes that were upregulated among 3,682 DEGs. Genes identified from each overlap are listed on the right side of the corresponding Venn diagram. The letter following each gene name indicates its type, with “A” representing aliphatic and “I” representing indolic GSLs. **G)** Venn diagram analysis showing the overlap between 78 *B. oleracea* GSL pathway genes and differentially expressed genes (DEGs) in AV samples compared with NV samples. The upper panel shows total 20 GSL pathway genes that were downregulated among 3,642 DEGs, while the lower panel shows 4 GSL pathway genes that were upregulated among 2,038 DEGs. Genes identified from each overlap are listed on the right side of the corresponding Venn diagram. The letter following each gene name indicates its type, with “A” representing aliphatic and “I” representing indolic GSLs.

Figure 4.

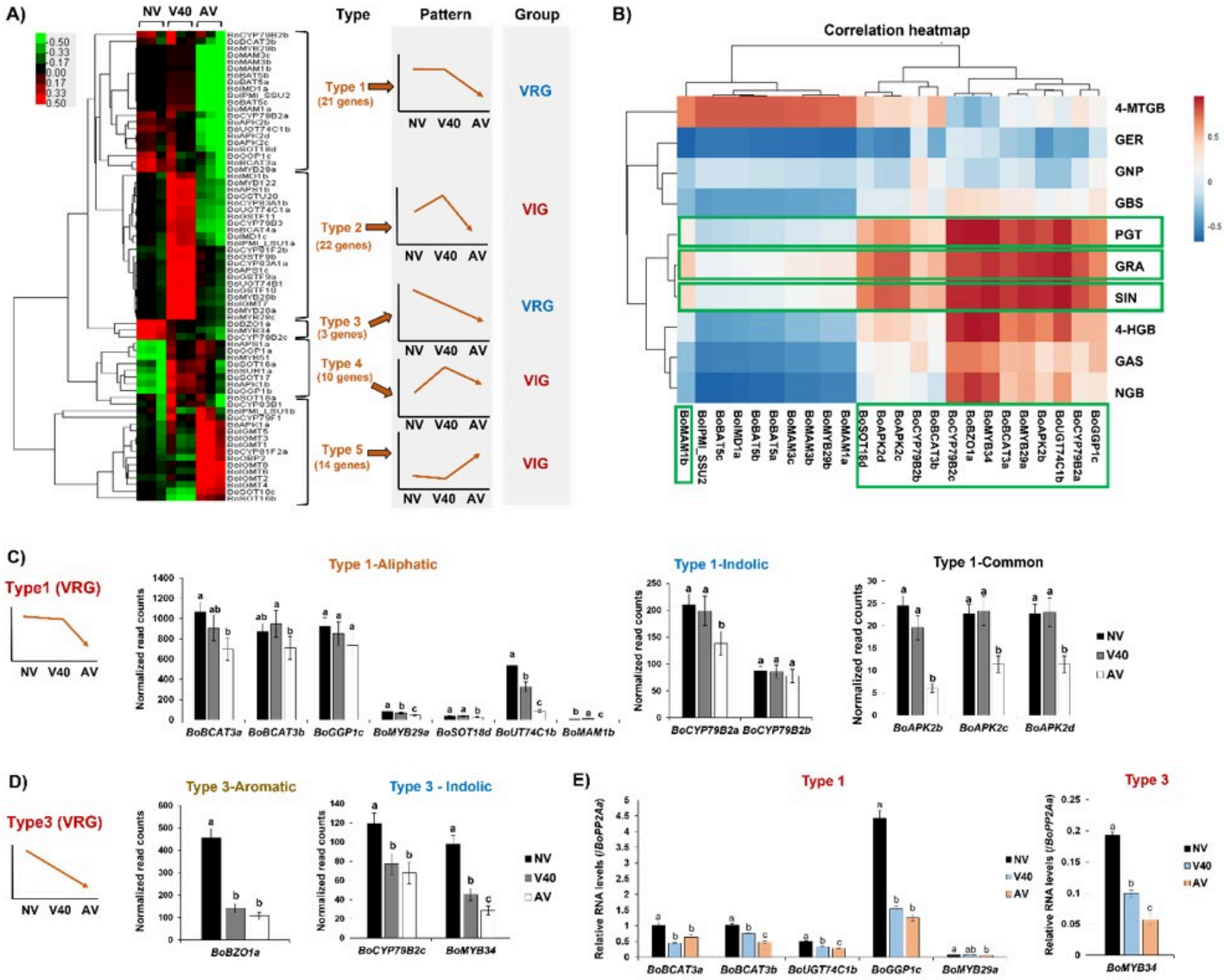

Figure 4

Correlation analysis between 10 GSL compounds profiles and transcriptional profile of GSL pathway genes along vernalization time course. A) A heatmap showing transcriptional profile of 70 GSL pathway genes during three vernalization time course (NV, V40, and AV) in *Brassica oleracea.* Based on the pattern of expression, 70 genes were divided into five types (Type1~Type 5). Total 21, 22, 3, 10, and 14 genes were included into each Type 1 ~ Type 5, respectively. These five different types were further classified into two groups, VRGs (Vernalization-Repressed GSL genes) and VIGs (Vernalization-Induced GSL genes) group. VRGs group contains genes belonging to Type 1 (21 genes) and Type 3 (3 genes), thus having total 24 genes. VIGs group contains genes belonging to Type 2 (22), Type 4 (10), and Type 5 (14), thus having a total of 46 genes. During the generation of this heatmap, 8 genes out of total 78 GSL pathway genes were filtered out due to low expression or low quality of p-value. **B)** a correlation heamap between the 10 GSL compound profiles and 24 VRGs group genes along vernalization time course**.** Total

15 VRG group genes were significantly correlated with three aliphatic GSL compounds like PGT, GRA, SIN profiles along vernalization (indicated with green line box on the bottom of the heatmap). These 15 VRG group genes (*BoMAM1b, BoSOT18d, BoAPK2d, BoAPK2c, BoCYP79B2b, BoBCAT3b, BoCYP79B2c, BoBZO1a, BoMYB34, BoBCAT3a, BoAPK2b, BoUGT74C1b, BoCYP79B2a* and *BoGGP1c*). **C)** Normalized transcript levels of 12 'Type 1' genes (*BoMAM1b*, *BoBCAT3a, BoBCAT3b, BoGGP1c, BoMYB29a, BoSOT18d, BoUT74C1b, BoCYP79B2a, BoCYP79B2b, BoAPK2b, BoAPK2c,* and *BoAPK2d*) belonging to VRG group showing a significant correlation with three aliphatic GSL compounds like PGT, GRA, SIN profiles along vernalization time course. **D)** Normalized transcript levels of three 'Type 3' genes (*BoBZO1a, BoCYP79B2c* and *BoMYB34*) belonging to VRG group showing a significant correlation with three aliphatic GSL compounds like PGT, GRA, SIN profiles along vernalization time course. **E)** Result of qRT-PCR analysis on five 'Type 1' genes (*BoBCAT3a, BoBCAT3b, BoUGT74C1b, BoGGP1c,* and *BoMYB29a*) and one 'Type 3' gene (*BoMYB34*) along vernalization time course. **C)~E)** Data were presented as mean ± standard deviation (SD) (n=3). Statistically significant differences were determined by one-way ANOVA and Tukey's post hoc test ($p < 0.05$).

Figure 5.

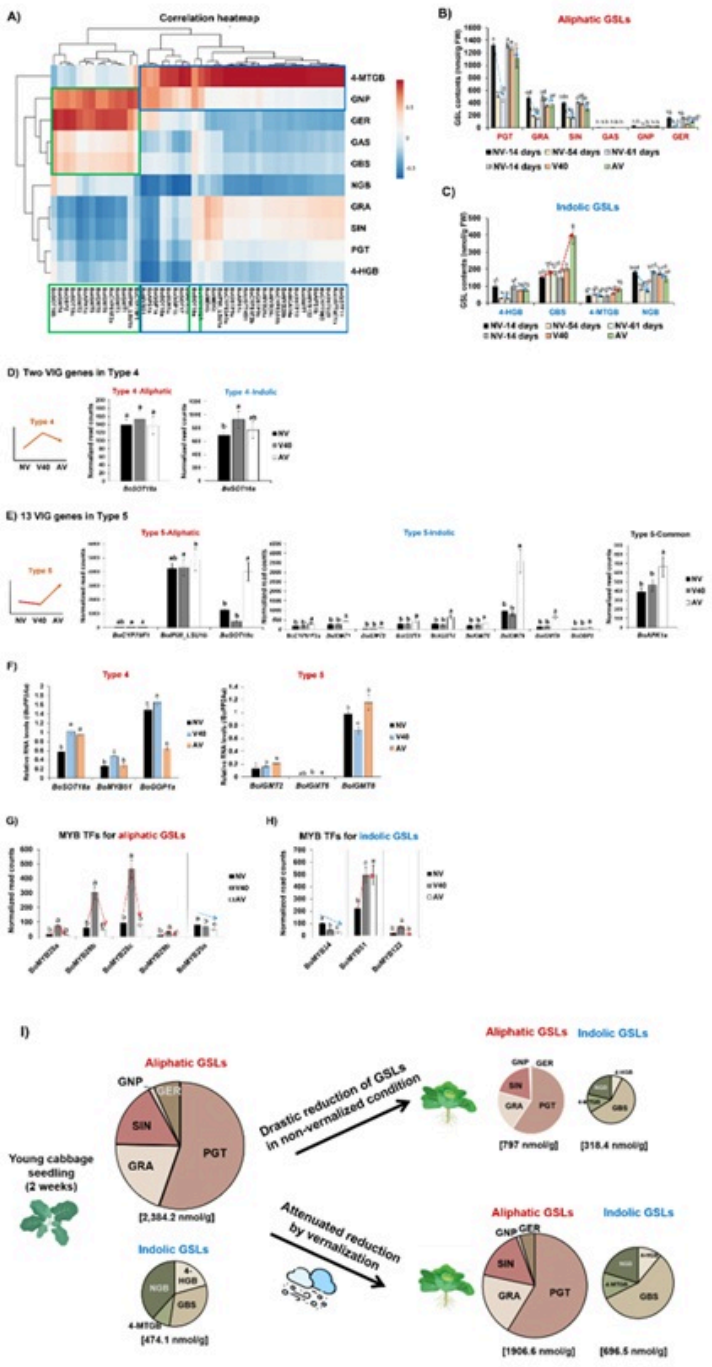

Figure 5

Vernalization attenudates drastic reduction of both aliphatic and indolic GSLs via transcriptional activation of VIG group genes. A) A correlation heamap between the 10 GSL compound profiles and 45 GSL pathway genes belonging to the Vernalization-Induction Genes (VIGs) group along vernalization time course**.** Some of VIG group genes were broadly correlated with 4-MTGB (indolic GSL) profile along vernalization (indicated with blue line box). In addition, total 15 VIG group genes were significantly

correlated with three aliphatic GSL compounds like GNP, GER, GAS, and GBS (indolic GSL) profiles along vernalization (indicated with green line box). These 15 VIG group genes were two 'Type 4' genes (*BoSOT18a* and *BoSOT16a*) and 13 'Type 5' genes (*BoCYP79F1, BoIPMI_LSU1b, BoSOT18c, BoCYP81F2a, BoIGMT1, BoIGMT2, BoIGMT3, BoIGMT4, BoIGMT5, BoIGMT6, BoIGMT8, BoOBP2*, and *BoAPK1a*) genes. **B)**Profiles of six aliphatic GSL compounds (PGT, GRA, SIN, GAS, GNP, and GER) between three non-vernalized (NV-14D, NV-54D, and NV-61D) and three vernalized (NV-14D, V40, and AV) time course. **C)** Profiles of four indolic GSL compounds (4-HGB, GBS, 4-MTGB, and NGB) between three non-vernalized (NV-14D, NV-54D, and NV-61D) and three vernalized (NV-14D, V40, and AV) time course. **D)** Normalized transcript levels of two genes (*BoSOT18a*and *BoSOT16a*) belonging to 'Type 4' group showing a significant correlation with GBS, a indolic GSL compount profile along vernalization. **E)**Normalized transcript levels of 13 genes (*BoCYP79F1, BoIPMI_LSU1b, BoSOT18c, BoCYP81F2a, BoIGMT1, BoIGMT2, BoIGMT3, BoIGMT4, BoIGMT5, BoIGMT6, BoIGMT8, BoOBP2*, and *BoAPK1a*) belonging to 'Type 5' group showing a significant correlation with GBS profile along vernalization. **F)** Result of qRT-PCR analysis on two genes (*BoSOT18a*and *BoSOT16a*) belonging to 'Type 4' group and three genes (*BoIGMT2*, *BoIGMT6*, and *BoIGMT8*) belonging to 'Type 5' showing a significant correlation with GBS, a indolic GSL compount profile along vernalization. **G)**Normalized transcript levels of 5 MYB TFs for aliphatic GSLs (*BoMYB28a*, *BoMYB28b*, *BoMYB28c*, *BoMYB29b*, and *BoMYB29a*). **H)**Normalized transcript levels of 3 MYB TFs for indolic GSLs (*BoMYB34*, *BoMYB51*, and *BoMYB122*). **B)-H)** Data were presented as mean ± standard deviation (SD) (n=3). Statistically significant differences were determined by one-way ANOVA and Tukey's post hoc test ($p < 0.05$). **I)** A schematic model illustrating changes in GSL profiles in cabbage with and without vernalization. Young cabbage seedlings (2 weeks old) contained high levels of aliphatic (2,384.2 nmol·g^{-1}) and indolic GSLs (474.1 nmol·g^{-1}). As plants aged, in the absence of vernalization, both aliphatic (797.0 nmol·g^{-1}) and indolic GSLs (318.4 nmol·g^{-1}) showed a substantial decline. In contrast, vernalization markedly attenuated the reduction of aliphatic GSLs (1,906.6 nmol·g^{-1}), and the total amount of indolic GSLs even increased following vernalization (696.5 nmol·g^{-1}). The size of each pie chart is proportional to the total amount of aliphatic or indolic GSLs. The total contents of aliphatic or indolic GSLs are indicated below each pie chart in parentheses. Progoitrin (PGT); Glucoraphanin (GRA); Sinigrin (SIN); Gluconapin (GNP); 4-Hydroxyglucobrassicin (4-HGB); Glucoerucin (GER); Glucobrassicin (GBS); 4-Methoxyglucobrassicin (4-MTGB); Neoglucobrassicin (NGB).

Supplementary Files

This is a list of supplementary files associated with this preprint. Click to download.

- SupplementaryTableS3.xlsx
- SupplementaryInformation.docx